Chapter 7

Sonochemical Degradation of Perfluorooctane Sulfonate (PFOS) and Perfluorooctanoate (PFOA) in Groundwater: Kinetic Effects of Matrix Inorganics*

7.1 Abstract

Ultrasonic irradiation has been shown to effectively degrade perfluorinated chemicals (PFCs) such as perfluorooctane sulfonate (PFOS) and perfluorooctanoate (PFOA) in aqueous solution. Reduced PFC sonochemical degradation rates in organic-rich groundwater taken from beneath a landfill, however, testify to the negative kinetic effects of the organic groundwater constituents. In this study, the PFOX (X = S or A) sonochemical degradation rates in a groundwater sample with organic concentrations 10 times lower than those in the groundwater taken from beneath a landfill are found to be 29.7% and 20.5% lower, respectively, than the rates in MilliQ water, suggesting that inorganic groundwater constituents also negatively affect PFC sonochemical kinetics. To determine the source of the groundwater matrix effects, we evaluate the effects of various inorganic species on PFOX sonochemical kinetics. Anions over the range of 1-10 mM show Hofmeister effects on the sonochemical degradation rates of PFOX, $k_{ClO_4^-}^{\text{-PFOX}} > k_{NO_3^-}^{\text{-PFOX}} \sim k_{Cl^-}^{\text{-PFOX}} \geq k_{MQ}^{\text{-PFOX}} > k_{HCO_3^-}^{\text{-PFOX}} \sim k_{SO_4^{2-}}^{\text{-PFOX}}$. In contrast, common cations at 5 mM have negligible effects. Initial solution pH enhances the degradation rates of PFOX at 3, but has negligible effects over the range of 4 to 11. The observed inorganic effects on sonochemical kinetics are hypothesized to be due to ions' partitioning to and interaction with the bubble-water interface. Finally, it is shown that the rate reduction in the groundwater in this study is primarily due to the presence of bicarbonate and thus can be fully rectified by pH adjustment prior to sonolysis.

7.2 Introduction

Perfluorinated chemicals (PFCs) such as perfluorooctane sulfonate (PFOS) and perfluorooctanoate (PFOA) have been manufactured for use in a variety of industrial and consumer applications.[1-2] Due to their environmental persistence, PFOX (X= S or A) have been detected in surface waters at a number of locations at concentrations ranging from pg L^{-1} to low ng L^{-1}.[3-6] Elevated concentrations (on the order of mg L^{-1}) of PFOX have been measured in surface and ground waters near specific point sources.[7-11]

PFOX are chemically inert due to the strength of the C-F bonds, and there is no direct evidence to date of their biodegradation.[12-13] PFOX cannot be removed by conventional water and wastewater treatment processes that do not utilize activated carbon adsorption or reverse osmosis.[13-15] Various treatment techniques have been proposed to abiotically decompose aqueous PFOX, including direct UV photolysis,[16] thermal- or UV-activated persulfate oxidation,[17-18] reductive defluorination using elemental iron at subcritical water conditions,[19] UV-iodide reduction,[20] B_{12}-mediated reduction,[21] and ultrasonic irradiation.[22] It is shown that ultrasonic irradiation can effectively degrade perfluoroalkylsulfonates such as PFOS and perfluoroalkylcarboxylates such as PFOA via pyrolysis under transient high temperatures at the bubble-water interface.[23] Advantages of the sonochemical degradation of PFOX include fast and complete mineralization of PFOX and a wide effective concentration range.[24]

It is important to understand the various environmental matrix effects on PFCs sonochemical degradation in order to better evaluate the prospect of its environmental applications. Our previous study on the sonochemical decomposition of PFOX in organic-rich groundwater taken from beneath a landfill has suggested that volatile

organic constituents decrease the sonochemical degradation rates of PFOX by reducing the average cavitation temperature at the bubble-water interface. Surface-active organic compounds may also compromise the sonochemical degradation efficiency via competitive adsorption onto the bubble-water interface. The rate reductions can be rectified by simultaneous application of ozonation and ultrasonic irradiation.[25]

Herein, we now report on the sonochemical degradation kinetics of PFOX in a distinctively different groundwater sample with a 10-fold lower total organic concentration (TOC) and a much higher electrolyte concentration. We extend the discussion of environmental matrix effects on PFC sonochemical degradation kinetics to include the inorganic ions most commonly found in surface and ground waters. A more comprehensive scheme of matrix effects will enable engineering improvements on the sonochemical degradation efficiency of PFOX in a variety of environmental waters.

7.3 Experimental Methods

Materials. Ammonium perfluorooctanoate (APFO) and potassium perfluorooctane sulfonate (PFOS-K^+) standards were provided by 3M. The sodium salts of chloride, nitrate, perchlorate, sulfate, and bicarbonate, ammonium chloride, magnesium chloride, and calcium chloride (Sigma Aldrich, 99% or higher purity) were used as received. Sep-Pak Vac tC18 (6 cc, 1 g) solid phase extraction (SPE) cartridges were purchased from Waters. Purified water (18.2 MΩ cm^{-1} resistivity) was prepared from a Millipore MilliQ Gradient water purification system.

Sonolysis. The sonochemical degradation kinetics of PFOX was measured in MilliQ, aqueous electrolyte solutions, and groundwater. Ultrasonication was performed in a 600

mL jacketed glass reactor at a frequency of 612 or 354 kHz using an Allied Signal - ELAC Nautik ultrasonic transducer. The applied power density was 250 W L^{-1} with an average energy transfer efficiency of 72 ± 5% as determined by calorimetry. The PFOX solutions were maintained at 10 ± 2 ºC by water cooling and sparged with argon 30 minutes prior to and during the course of the reaction. In all experiments the initial concentrations of PFOS and PFOA were spiked to approximately 100 μg L^{-1}, or 200 nM and 240 nM, respectively.

Solid Phase Extraction for Groundwater Samples. Groundwater samples taken during the sonochemical reactions were purified by SPE using Sep-Pak Vac tC18 cartridges (6 cc, 1 g) to remove matrix components that may interfere with the LC/MS analysis. The SPE cartridges were conditioned by passing 10 mL methanol, and then 50 mL water through the cartridges at a flow rate of 2 mL min^{-1}. The analytical samples were subsequently loaded onto the wet cartridges at 1 mL min^{-1}. The columns were dried with nitrogen gas for 5 minutes, rinsed with 10 mL 20% methanol in water at 2 mL min^{-1}, and dried with nitrogen gas for another 30 minutes. The analytes were eluted with methanol at 1 mL min^{-1}, and 4.0 mL samples were collected into 14 mL polypropylene tubes (Falcon). The recovery rates of PFOX were above 90%, consistent with literature values.[26] All steps except sample loading were performed on a Caliper AutoTrace SPE Work Station.

LC/MS Analyses. The PFOX concentrations were quantified by LC/MS. For MilliQ and electrolyte solutions, sample aliquots (700 μL) were withdrawn from the reactor using disposable plastic syringes, transferred into 750 μL polypropylene autosampler vials, and sealed with PTFE septum crimp caps (Agilent). Groundwater samples were

purified by SPE before they were transferred to the autosampler vials. 20 μL of samples were injected into an Agilent 1100 HPLC for separation on a Thermo-Electron Betasil C18 column (100 mm × 2.1 mm, 5 μm). The flow rate was maintained at 0.3 mL min^{-1} with a mobile phase of 2 mM ammonium acetate in water (A) and methanol (B). The eluent gradient started with 5% B over the first minute, was ramped to 90% B over 10 minutes and held for 2.5 minutes, then ramped back to 5% B over 0.5 minute and held for 3 minutes, and finished with a 3 minute post-time. Chromatographically separated samples were analyzed by an Agilent Ion Trap in negative mode monitoring for the perfluorooctanesulfonate molecular ion (*m/z* = 499) and the decarboxylated perfluorooctanoate (*m/z* = 369). Instrumental parameters were set at the following levels: nebulizer pressure 40 PSI, drying gas flow rate 9 L min^{-1}, drying gas temperature 325 ºC, capillary voltage +3500 V, and skimmer voltage –15 V. Quantification was based on a 8-point calibration curve spanning the 1 to 200 μg L^{-1} range fitted to a quadratic with X^{-1} weighting. Analytical standards, quality control, and reagent blank samples were included in each analytical batch along with the unknown samples. Further analytical details were described in a previous paper.[23]

7.4 Results

Groundwater Characterization. The groundwater used in the study was sampled from a well in the city of Oakdale, MN. The groundwater sample was stored in darkness at 4°C in a sealed container with minimal headspace. As summarized in Table 7.1, the TOC concentration of the groundwater sample is 1.5 mg L^{-1}, about an order of magnitude lower than that of groundwater taken from beneath a landfill that was used in our previous study,[25] whereas the concentrations of common groundwater ions such as

bicarbonate, sulfate, chloride, calcium, and magnesium are much higher than in the previous study. PFOX were spiked into the groundwater to increase the concentration to approximately 100 μg L^{-1}, or 200 and 240 nM for PFOS and PFOA, respectively.

Sonolysis of Groundwater PFOS and PFOA. The sonochemical degradation kinetics of PFOX in groundwater and MilliQ water are shown in Figure 7.1a and b, respectively (f = 612 kHz, PD = 250 W L^{-1}, T = 10 ^{o}C, argon). The sonochemical degradation of groundwater PFOX follows pseudo-first-order kinetics as is observed in MilliQ. However, the pseudo-first-order rate constant for groundwater PFOS at 612 kHz, k_{GW}^{-PFOS} = 0.0135 min^{-1}, is 70.3% of the MilliQ rate constant, k_{MQ}^{-PFOS} = 0.0192 min^{-1}. Similar results are observed for PFOA, where the rate constant for groundwater PFOA, k_{GW}^{-PFOA} = 0.0291 min^{-1}, is 79.5% of the MilliQ rate constant, k_{MQ}^{-PFOA} = 0.0366 min^{-1}. At a frequency of 354 kHz, a similar reduction in rate constant is observed when comparing sonolysis in MilliQ versus in groundwater (Figure 7.6).

Sonolysis of PFOS and PFOA in Aqueous Electrolyte Solutions. In order to evaluate the electrolytes most responsible for the rate reduction in the groundwater sample, the sonochemical degradation kinetics of PFOX in selected aqueous electrolyte solutions were evaluated under the same sonolysis conditions as in previous experiments. Figure 7.2a and b shows the concentration-dependent effect of 1-10 mM Na_2SO_4, $NaHCO_3$, NaCl, $NaNO_3$, or $NaClO_4$ on the sonochemical degradation rates of PFOX. The sonochemical rate constants for PFOX increase steadily as the concentration of $NaClO_4$ increases from 0 to 10 mM, with the rate enhancement at 10 mM being 47% for PFOS and 11% for PFOA. In aqueous solutions of $NaNO_3$ and NaCl, the sonochemical

degradation rates for PFOS are moderately enhanced, whereas those for PFOA are identical within experimental error to the MilliQ rate. $NaHCO_3$ and Na_2SO_4 are found to reduce the sonochemical rate constants for PFOX. Thus, with Na^+ being the common cation, the overall effect of anions on the differential sonochemical degradation rate constants relative to those in MilliQ for PFOX, $\Delta k_i^{\text{-PFOX}} = k_i^{\text{-PFOX}} - k_{\text{MQ}}^{\text{-PFOX}}$, follows the order: $\Delta k_{ClO_4^-}^{\text{-PFOX}} > \Delta k_{NO_3^-}^{\text{-PFOX}} \sim \Delta k_{Cl^-}^{\text{-PFOX}} \geq 0 > \Delta k_{HCO_3^-}^{\text{-PFOX}} > \Delta k_{SO_4^{2-}}^{\text{-PFOX}}$. The negative effects of SO_4^{2-} and HCO_3^- on PFOA degradation rates are of similar magnitude. This order is consistent with the Hofmeister series, which was initially observed for specific ion effects on protein solubility and now has been extended to a number of other systems including ion partitioning between bulk water and the air-water interface.[27-28] It is also of note that the specific anion effects on the sonochemical degradation rates, though similar in order, are greater for PFOS than for PFOA.

In contrast, the effect of cations on the sonochemical degradation rates of PFOX is much less pronounced than that of anions over the same concentration range. As shown in Figure 7.3, no significant difference in sonochemical rate constant is observed in aqueous solutions of NaCl and NH_4Cl at 5 mM and of $CaCl_2$ and $MgCl_2$ at 2.5 mM.

The effect of solution pH, as adjusted by addition of NaOH or HCl, on the sonochemical degradation rates of PFOX in MilliQ water was also examined. As is shown in Figure 7.4, the sonochemical rate constants remain unchanged within experimental error as a function of pH over the range of 4 to 11. At pH 3, the rate constants increase by 23.4% and 13.7% for PFOS and PFOA, respectively, relative to those in MilliQ water at pH 7. For comparison, the rate enhancement in the 1 mM HCl solution is significantly greater than that in the 1 mM NaCl solution, indicating the role of

increased proton concentration. Also, acidification increases the degradation rate of PFOS to a greater extent, consistent with the effect of anions reported in this text as well as that of organics reported in our previous study.[25] Together, these suggest that PFOS sonochemical kinetics is more susceptible to matrix effects.

Sonolysis of PFOS and PFOA in Groundwater after pH Adjustment. Given that bicarbonate (pK_1 = 6.3, pK_2 = 10.3), at approximately 2.2 mM, is the primary anionic component of the groundwater sample, we evaluated the effect of bicarbonate removal by pH adjustment, both acidification and alkalization, on the sonochemical degradation rates of PFOX, as shown in Figure 7.5a and b. Sonolysis conditions were the same as in previous experiments. For the alkalization experiments, the groundwater pH was adjusted from its initial value of 8.0 to 11.0 by NaOH and the white $CaCO_3$ precipitate thus formed was removed by filtration. The PFOS and PFOA sonochemical rate constants in the alkaline groundwater supernatant are rectified to 101.0% and 94.0%, respectively, of the MilliQ rates. For the acidification experiments, the groundwater was acidified to pH 3.9 by HCl to convert bicarbonate to carbon dioxide (titration curve shown in Figure 7.7), which was then removed from solution by bubbling with argon. The acidification may also have removed volatile organic acids from the groundwater through a similar mechanism. The sonochemical degradation rates are enhanced to 133.9% for PFOS and 104.4% for PFOA relative to the MilliQ rates. Both experiments suggest that bicarbonate is primarily responsible for the reduction in PFOX sonochemical kinetics in the groundwater in this study.

7.5 Discussion

A sonochemical kinetic model is defined and utilized to better understand the specific ion effects observed in Figures 7.2 to 7.4. Assuming that interfacial pyrolysis is the only viable sonochemical degradation pathway for PFOX, and that adsorption to the bubble-water interface is required for interfacial pyrolysis to occur,[23] the sonochemical degradation rate of PFOX can be expressed as eq. (7.1).

$$\frac{d[\mathrm{PFOX}]}{dt} = -k_{app}^{-\mathrm{PFOX}}[\mathrm{PFOX}] = -k_{\Delta}^{-\mathrm{PFOX}}\theta^{\mathrm{PFOX}} \tag{7.1}$$

k_{app}^{-PFOX} is the apparent pseudo first-order rate constant, k_{Δ}^{-PFOX} the maximum absolute rate, i.e., the pyrolytic unimolecular decomposition rate attained when all of the transiently cavitating bubble surface sites are occupied by PFOX molecules, and θ^{PFOX} the fraction of bubble-water interface sites occupied by PFOX molecules. k_{Δ}^{-PFOX} is defined by eq. (7.2).

$$k_{\Delta}^{-\mathrm{PFOX}} = [S]A^{\mathrm{PFOX}} \exp\left(-E_A^{\mathrm{PFOX}} / R\left\langle T_{\mathrm{int}}^{bub}\right\rangle\right) \tag{7.2}$$

where [S] is the molarity of transiently cavitating bubble-water interfacial sites, A^{PFOX} the preexponential constant in s^{-1}, E_A^{PFOX} the activation energy for the pyrolytic cleavage of the ionic head group of PFOX in kJ mol^{-1},[29-30] and $\left\langle T_{\mathrm{int}}^{bub}\right\rangle$ the average interfacial temperature during the high-temperature period of a transient bubble collapse.[31-32] In the presence of other matrix components that may compete for bubble-water interfacial sites, θ^{PFOX} is represented by eq. (7.3).

$$\theta^{\mathrm{PFOX}} = \frac{K^{\mathrm{PFOX}}[\mathrm{PFOX}]}{1 + K^{\mathrm{PFOX}}[\mathrm{PFOX}] + \sum_i K^i[i]} \tag{7.3}$$

K^i is the bulk water to air-water interface partitioning coefficient for species *i*. It has been observed that sonochemical partitioning coefficients, $K_{\text{sono}}^{\text{PFOX}}$, are enhanced over equilibrium partitioning coefficients, $K_{\text{eq}}^{\text{PFOX}}$, due to high-velocity radial bubble oscillations.[24]

Our previous study on the effect of groundwater taken from beneath a landfill on PFOX sonochemical kinetics suggests that matrix organics may reduce PFOX degradation kinetics through reduction both in $\left\langle T_{\text{int}}^{bub} \right\rangle$ due to energy consumption by volatile organics in the bubble vapor phase, and in θ^{PFOX} due to competition for bubble-water interfacial sites by surface-active organics.[25] As for aqueous electrolyte solutions, since ions cannot partition to the bubble vapor phase, temperature effects, if present, should be caused by other mechanisms. Given that the more surface active ClO_4^- actually increases the PFOX degradation rates whereas the less surface active SO_4^{2-} and HCO_3^- reduce the PFOX degradation rates, the surface competition effect is minimal, i.e., $\sum_i K^i[i] << 1$ in eq. (7.3).

Addition of electrolytes such as NaCl has been reported to enhance both the sonoluminescence intensity[33-34] and the sonochemical degradation rates of compounds such as phenol and 2,4-dinitrophenol.[35-36] The enhancement has been explained by the effect of electrolytes on gas solubility in aqueous solution and by the "salting out" effect that increases the concentration of organics at the bubble-water interface, respectively. However, both effects were observed at significantly higher electrolyte concentrations than those used in this study.

Observations that anions have both positive and negative effects on PFOX sonochemical kinetics indicate specific ion effects. Relative anionic effects on PFOX sonochemical kinetics (Figure 7.2) follow the Hofmeister series. We hypothesize that these effects are correlated to the ion partitioning between the bulk water and the bubble-water interface, which will affect bubble-water interfacial properties such as surface potential and interfacial water structure. For example, ClO_4^- is highly enriched at the air-water interface relative to the bulk solution,[28] and therefore yields a more negatively charged bubble-water interface. The increase in negative surface potential at the bubble-water interface enhances electrostatic repulsion between cavitating bubbles, thus reducing their propensity to coalesce.[37] This further results in a population of smaller bubbles with greater surface area to volume ratio and thus a greater number of surface sites available for PFOX pyrolysis, i.e., greater [*S*] in eq. (7.2). Well hydrated and thus less surface active anions such as SO_4^{2-} will reduce the negative potential at the bubble-water interface. The results in Figure 7.2 are qualitatively consistent with measured surface potentials of various aqueous electrolyte solutions.[38]

A quantitative explanation based on the surface potential measurements is difficult to establish, not only because the exact relationship between [*S*] and bubble-water interfacial potential is unclear, but also because surface potential measurements yield equilibrium air-water interface partitioning values, whereas ion partitioning to the ultrasonically cavitating bubble interface is kinetically constrained. Cavitating bubble lifetimes (100 μs) are much shorter than ion partitioning half-lives (>1 ms), and high-velocity bubble radial oscillations will dominate over chemical diffusion. Thus, relative

differences in equilibrium surface potential can only be used as a rough guideline for adsorption processes at acoustically cavitating bubble interfaces.

In addition, the observed anionic effects on PFOX sonochemical kinetics may also be due to the effect of anions on the interfacial water structure. The propensity of anions to orient interfacial water has been observed to follow the Hofmeister series: $NaClO_4$ > $NaNO_3$ > NaCl > pure water > Na_2SO_4.[39] Altering the interfacial water structure may affect the amount of water vapor transported into the bubble, and thus $\left\langle T_{\text{int}}^{bub} \right\rangle$. Alterations in water structure and composition at the bubble-water interface may also affect heat transfer from the bubble vapor to the bulk liquid. The resulting changes in average bubble-water interfacial temperatures during transient cavitation will subsequently affect the observed sonochemical rates of PFOX degradation.

The negligible effect of cations on PFOX sonochemical kinetics, as shown in Figure 7.3, is likely due to their much greater degree of hydration that limits their interactions with the sonochemically active bubble-water interface. This is consistent with observations in other systems that the Hofmeister effects of small cations, if present, are much smaller in magnitude than those of anion.[39-41]

The enhanced PFOX sonochemical kinetics at pH below 4 may also result from the interactions of proton with the bubble-water interface. The interface is believed to become increasingly positively charged as the pH drops below 4, despite the uncertainty over the extent of proton and hydroxide enhancement at the bubble-water interface.[42-43] The increasingly positive surface charge may not only reduce bubble coalescence, thus increasing [*S*] in eq. (7.2), but also attract more of the oppositely charged PFOX to the surface, thus increasing θ^{PFOX} in eq. (7.3). It is also of note that at pH 3, PFOA may form

a $(PFO)_2H^-$ cluster, which may affect the overall sonochemical degradation rate of PFOA.[44]

Bicarbonate, whose concentration in the groundwater sample is nearly 2 orders of magnitude greater than TOC, is likely to be the primary matrix component affecting PFOX sonochemical kinetics as shown in Figure 7.1. Indeed, the rate reduction in a 2 mM HCO_3^- aqueous solution as shown in Figure 7.2, $k_{HCO_3^-}^{-PFOS} / k_{MQ}^{-PFOS} = 0.82$ and $k_{HCO_3^-}^{-PFOA} / k_{MQ}^{-PFOA} = 0.86$, does account for a major part of the rate reduction observed in the groundwater, $k_{GS}^{-PFOS} / k_{MQ}^{-PFOS} = 0.70$ and $k_{GS}^{-PFOA} / k_{MQ}^{-PFOA} = 0.80$. Since the primary sonochemical degradation mechanism for PFOX is interfacial pyrolysis, the effect of bicarbonate on PFOX sonochemical kinetics is likely due to its impact on the interfacial pyrolysis conditions. The effect of bicarbonate as OH radical scavenger, while having been shown in general to reduce sonochemical degradation rates,[45] is inconsequential in this case, because the reaction of PFOX with OH radical is slow.[23] Other groundwater matrix components such as sulfate and organic compounds may have minor impacts on the sonochemical degradation rates of PFOX.

The sonochemical degradation rates post-acidification are even higher than the MilliQ rates, presumably due to a combination of factors including the effect of pH and Cl^-. First, at pH 3.9 the sonochemical degradation rates may be slightly enhanced. Second, the addition of 2.5 mM Cl^- to adjust pH may also increase the degradation rates, but as shown in Figure 7.2, the rate enhancement in MilliQ upon addition of 2 mM Cl^- is smaller than 5%. Since both factors combined cannot fully account for the observed rate enhancement, synergistic effects from the groundwater matrix are likely to be present.

The observed reduction in PFOX sonochemical degradation rates in groundwater relative to MilliQ rates in the range of 20%–30% is moderate considering the relative concentrations of PFOX (100 μg L^{-1}) to the various groundwater components: on a mass basis, TOC / [PFOX] = 15, [SO_4^{2-}] / [PFOX] = 180, and [HCO_3^-] / [PFOX] = 1400. It is found in our previous study that even in a groundwater with TOC / [PFOX] > 100, the sonochemical PFOX degradation rates are decreased by no more than 60%. Some other oxidative or reductive degradation methods[46] may be more significantly affected by matrix compounds at these concentrations, since reactions rates with these compounds greatly exceed reaction rates with PFOX. In the example of UV-persulfate oxidation where PFOX is effectively degraded by reaction with sulfate anion radical, the matrix effect of HCO_3^- is expected to be much more significant because sulfate anion radical reacts with PFOX with a second-order rate constant of 10^4 M^{-1} s^{-1} and with HCO_3^- with a second-order rate constant of 9×10^6 M^{-1} s^{-1}.[47-48] Finally, the decrease in PFOX sonochemical degradation rates due to bicarbonate can be effectively rectified by a simple pH adjustment. Both alkalization and acidification have been observed to rectify rates to at least those observed in MilliQ, with acidification even amplifying rates over those expectations.

7.6 Acknowledgements

The authors would like to thank 3M for the financial support and Dr. Nathan Dalleska and the Caltech Environmental Analysis Center for technical assistance in sample analysis.

7.7 References

(1) Houde, M.; Martin, J. W.; Letcher, R. J.; Solomon, K. R.; Muir, D. C. G., *Environ. Sci. Technol.* **2006,** *40*, 3463-3473.

(2) Prevedouros, K.; Cousins, I. T.; Buck, R. C.; Korzeniowski, S. H., *Environ. Sci. Technol.* **2006**, *40*, 32-44.

(3) So, M. K.; Taniyasu, S.; Yamashita, N.; Giesy, J. P.; Zheng, J.; Fang, Z.; Im, S. H.; Lam, P. K. S., *Environ. Sci. Technol*. **2004**, *38*, 4056-4063.

(4) Murakami, M.; Imamura, E.; Shinohara, H.; Kiri, K.; Muramatsu, Y.; Harada, A.; Takada, H., *Environ. Sci. Technol.* **2008,** *42*, 6566-6572.

(5) Furdui, V. I.; Helm, P. A.; Crozier, P. W.; Lucaciu, C.; Reiner, E. J.; Marvin, C. H.; Whittle, D. M.; Mabury, S. A.; Tomy, G. T., *Environ. Sci. Technol.* **2008,** *42*, 4739-4744.

(6) Yamashita, N.; Kannan, K.; Taniyasu, S.; Horii, Y.; Petrick, G.; Gamo, T. In *A Global Survey of Perfluorinated Acids in Oceans*, 2005; Pergamon-Elsevier Science Ltd: 2005; pp 658-668.

(7) Konwick, B. J.; Tomy, G. T.; Ismail, N.; Peterson, J. T.; Fauver, R. J.; Higginbotham, D.; Fisk, A. T., *Environ. Toxicol. Chem.* **2008,** *27*, 2011-2018.

(8) Clara, M.; Scheffknecht, C.; Scharf, S.; Weiss, S.; Gans, O., *Water Sci. Technol.* **2008,** *58*, 59-66.

(9) Oliaei, F. O.; Kriens, D.; Kessler, K. *Investigation of Perfluorochemical (PFC) Contamination in Minnesota Phase One*; Minnesota Pollution Control Agency: 2006.

(10) Schultz, M. M.; Barofsky, D. F.; Field, J. A., *Environ. Sci. Technol.* **2004,** *38*, 1828-1835.

(11) Moody, C. A.; Hebert, G. N.; Strauss, S. H.; Field, J. A., *J. Environ. Monit.* **2003,** *5*, 341-345.

(12) Key, B. D.; Howell, R. D.; Criddle, C. S., *Environ. Sci. Technol.* **1998,** *32*, 2283-2287.

(13) Schultz, M. M.; Higgins, C. P.; Huset, C. A.; Luthy, R. G.; Barofsky, D. F.; Field, J. A., *Environ. Sci. Technol.* **2006,** *40*, 7350-7357.

(14) Sinclair, E.; Kannan, K., *Environ. Sci. Technol.* **2006,** *40*, 1408-1414.

(15) Takagi, S.; Adachi, F.; Miyano, K.; Koizumi, Y.; Tanaka, H.; Mimura, M.; Watanabe, I.; Tanabe, S.; Kannan, K., *Chemosphere* **2008,** *72*, 1409-1412.

(16) Yamamoto, T.; Noma, Y.; Sakai, S. I.; Shibata, Y., *Environ. Sci. Technol.* **2007,** *41*, 5660-5665.

(17) Hori, H.; Nagaoka, Y.; Murayama, M.; Kutsuna, S., *Environ. Sci. Technol.* **2008,** *42*, 7438-7443.

(18) Hori, H.; Yamamoto, A.; Kutsuna, S., *Environ. Sci. Technol.* **2005,** *39*, 7692-7697.

(19) Hori, H.; Nagaoka, Y.; Yamamoto, A.; Sano, T.; Yamashita, N.; Taniyasu, S.; Kutsuna, S.; Osaka, I.; Arakawa, R., *Environ. Sci. Technol.* **2006,** *40*, 1049-1054.

(20) Park, H.; Vecitis, C. D.; Cheng, J.; Choi, W.; Mader, B. T.; Hoffmann, M. R., *J. Phys. Chem. A* **2009,** *113*, 690-696.

(21) Ochoa-Herrera, V.; Sierra-Alvarez, R.; Somogyi, A.; Jacobsen, N. E.; Wysocki, V. H.; Field, J., *Environ. Sci. Technol.* **2008,** *42*, 3260-3264.

(22) Moriwaki, H.; Takagi, Y.; Tanaka, M.; Tsuruho, K.; Okitsu, K.; Maeda, Y., *Environ. Sci. Technol.* **2005,** *39*, 3388-3392.

(23) Vecitis, C. D.; Park, H.; Cheng, J.; Mader, B. T.; Hoffmann, M. R., *J. Phys. Chem. A* **2008,** *112*, 4261-4270.

(24) Vecitis, C. D.; Park, H.; Cheng, J.; Mader, B. T.; Hoffmann, M. R., *J. Phys. Chem. C* **2008,** *112*, 16850-16857.

(25) Cheng, J.; Vecitis, C. D.; Park, H.; Mader, B. T.; Hoffmann, M. R., *Environ. Sci. Technol.* **2008,** *42*, 8057-8063.

(26) Hansen, K. J.; Johnson, H. O.; Eldridge, J. S.; Butenhoff, J. L.; Dick, L. A., *Environ. Sci. Technol.* **2002,** *36*, 1681-1685.

(27) Cacace, M. G.; Landau, E. M.; Ramsden, J. J., *Q. Rev. Biophys.* **1997,** *30*, 241-277.

(28) Cheng, J.; Vecitis, C. D.; Hoffmann, M. R.; Colussi, A. J., *J. Phys. Chem. B* **2006,** *110*, 25598-25602.

(29) Krusic, P. J.; Marchione, A. A.; Roe, D. C., *J. Fluor. Chem.* **2005,** *126*, 1510-1516.

(30) Krusic, P. J.; Roe, D. C., *Anal. Chem.* **2004,** *76*, 3800-3803.

(31) Kotronarou, A.; Mills, G.; Hoffmann, M. R., *J. Phys. Chem.* **1991,** *95*, 3630-3638.

(32) Suslick, K. S.; Hammerton, D. A.; Cline, R. E., *J. Am. Chem. Soc.* **1986,** *108*, 5641-5642.

(33) Wall, M.; Ashokkumar, M.; Tronson, R.; Grieser, F., *Ultrason. Sonochem.* **1999,** *6*, 7-14.

(34) Tronson, R.; Ashokkumar, M.; Grieser, F., *J. Phys. Chem. B* **2002,** *106*, 11064-11068.

(35) Mahamuni, N. N.; Pandit, A. B., *Ultrason. Sonochem.* **2006,** *13*, 165-174.

(36) Guo, Z. B.; Feng, R.; Li, J. H.; Zheng, Z.; Zheng, Y. F., *J. Hazard. Mater.* **2008,** *158*, 164-169.

(37) Sunartio, D.; Ashokkumar, M.; Grieser, F., *J. Am. Chem. Soc.* **2007,** *129*, 6031-6036.

(38) Jarvis, N. L.; Scheiman, M. A., *J. Phys. Chem.* **1968,** *72*, 74-&.

(39) Chen, X.; Yang, T.; Kataoka, S.; Cremer, P. S., *J. Am. Chem. Soc.* **2007,** *129*, 12272-12279.

(40) Piazza, R.; Pierno, M. In *Protein Interactions near Crystallization: A Microscopic Approach to the Hofmeister Series*, 2000; Iop Publishing: 2000; pp A443-A449.

(41) Fesinmeyer, R. M.; Hogan, S.; Saluja, A.; Brych, S. R.; Kras, E.; Narhi, L. O.; Brems, D. N.; Gokarn, Y. R., *Pharm. Res.* **2009,** *26*, 903-913.

(42) Beattie, J. K.; Djerdjev, A. N.; Warr, G. G., **2009,** *141*, 31-39.

(43) Winter, B.; Faubel, M.; Vacha, R.; Jungwirth, P., *Chem. Phys. Lett.* **2009,** *474*, 241-247.

(44) Cheng, J.; Psillakis, E.; Hoffmann, M. R.; Colussi, A. J., *J. Phys. Chem. A* **2009,** *113*, 8152-8156.

(45) Hung, H. M.; Kang, J. W.; Hoffmann, M. R., *Water Environ. Res.* **2002,** *74*, 545-556.

(46) Vecitis, C. D.; Park, H.; Cheng, J.; Mader, B. T.; Hoffmann, M. R., *Front. Environ. Sci. Eng. China* **2009,** *3*, 129-151.

(47) Kutsuna, S.; Hori, H., *Int. J. Chem. Kinet.* **2007,** *39*, 276-288.

(48) Neta, P.; Huie, R. E.; Ross, A. B., *J. Phys. Chem. Ref. Data* **1988,** *17*, 1027-1284.

Table 7.1, Primary components of the groundwater sample [a]

pH	7.9	Chloride, mg L^{-1} as Cl	14
Temperature, ºC	11.7	Nitrate-nitrite, mg L^{-1} as N	1.9
Dissolved oxygen, mg L^{-1}	6.3	Calcium, mg L^{-1} as Ca	64
TOC, mg L^{-1}	1.5	Magnesium, mg L^{-1} as Mg	20
Total suspended solids, mg L^{-1}	3.0	Sodium, mg L^{-1} as Na	7.3
Total alkalinity, mg L^{-1} as $CaCO_3$	220	Potassium, mg L^{-1} as K	1.0
Bicarbonate alkalinity, mg L-1 as $CaCO_3$	220	Iron, mg L^{-1} as Fe	<0.05
Sulfate, mg L^{-1} as SO_4	18	Manganese, mg L^{-1} as Mn	<0.01

a. Measurements completed by PACE Analytical

Figure 7.1. $\ln([PFOS]_t / [PFOS]_i)$ (a) and $\ln([PFOA]_t / [PFOA]_i)$ (b) vs. time in minutes during sonochemical degradation in MilliQ water (○) and groundwater (□). Reaction conditions are 612 kHz, 250 W L^{-1}, Ar, 10 °C, and $[PFOS]_i = [PFOA]_i = 100$ μg L^{-1}. Each error bar represents one standard deviation from the mean of at least three experiments. $k_{MQ}^{-PFOS} = 0.0192$ min^{-1}, $k_{GW}^{-PFOS} = 0.0135 min^{-1}$, $k_{MQ}^{-PFOA} = 0.0366$ min^{-1}, and $k_{GW}^{-PFOA} = 0.0291$ min^{-1}.

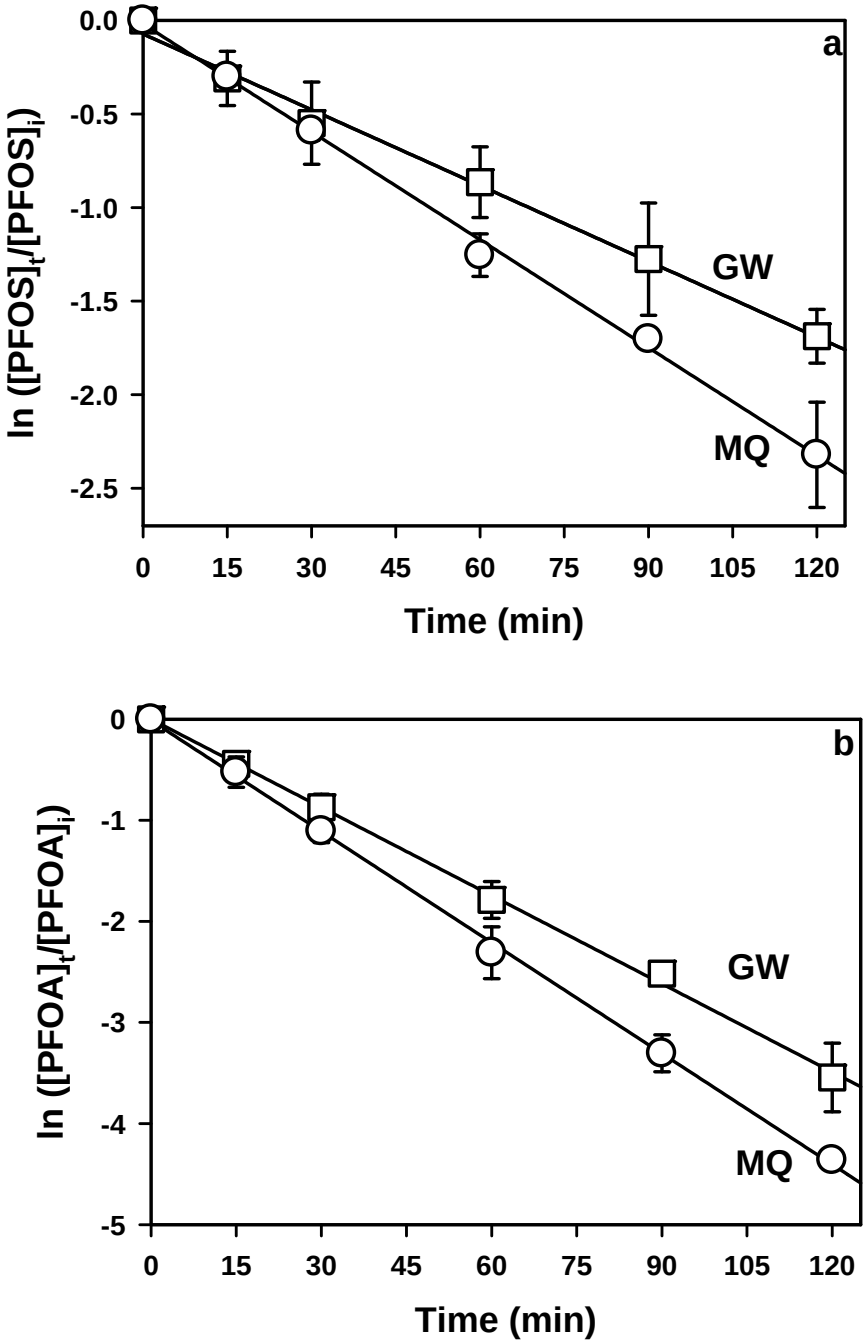

Figure 7.2. The observed pseudo-first-order rate constant normalized to the MilliQ rate constant, $k^{-PFOS} / k_{MQ}^{-PFOS}$ (a) and $k^{-PFOA} / k_{MQ}^{-PFOA}$ (b), vs. concentration of $NaClO_4$ (○), $NaNO_3$ (□), NaCl (△), Na_2SO_4(▽), and $NaHCO_3$(◇) in mM. Reaction conditions are 612 kHz, 250 W L^{-1}, Ar, 10 °C, and $[PFOS]_i = [PFOA]_i = 100$ μg L^{-1}.

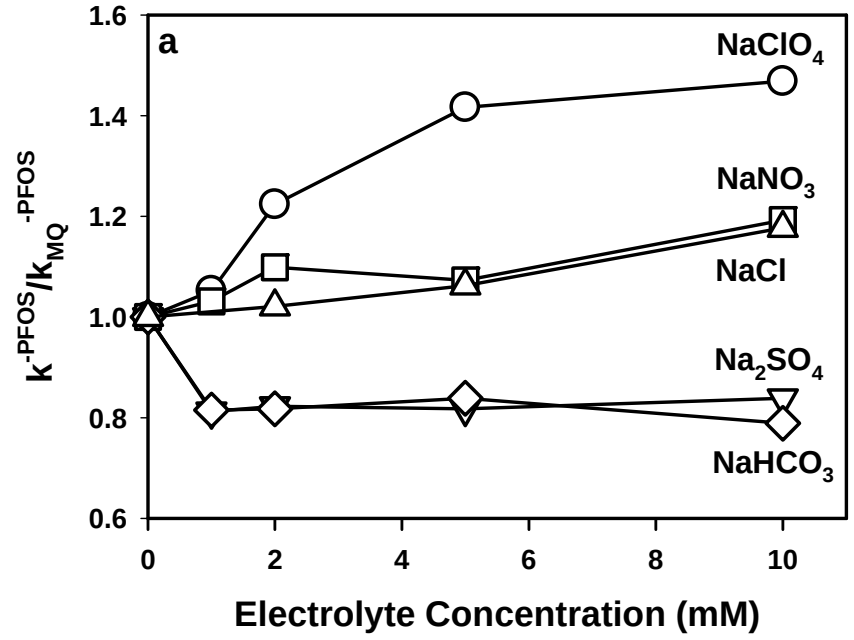

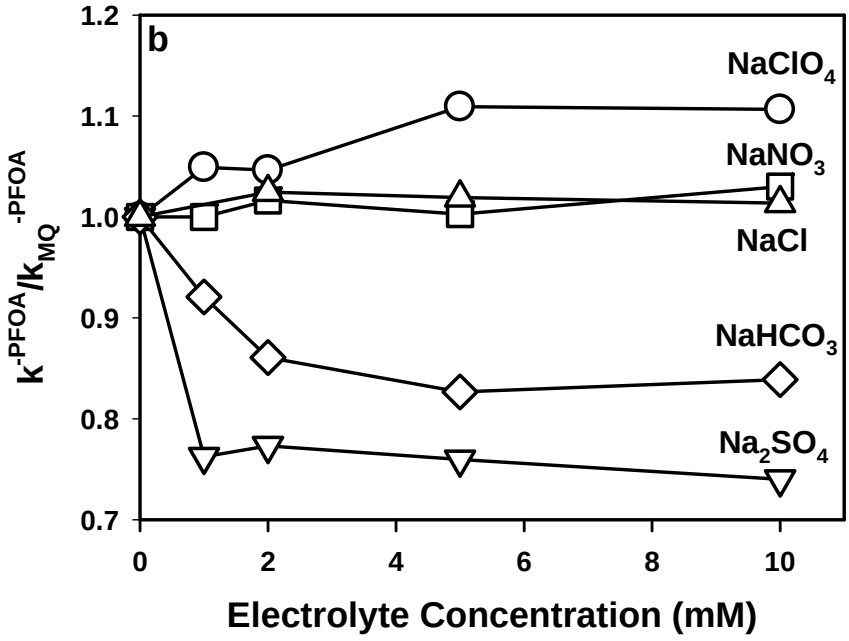

Figure 7.3. The observed pseudo-first-order rate constant for sonolysis of PFOA (clear bars) and PFOS (filled bars) in MilliQ water, aqueous solutions of 5mM NaCl, 5mM NH_4Cl, 2.5mM $CaCl_2$, and 2.5 mM $MgCl_2$. Reaction conditions are 612 kHz, 250 W L^{-1}, Ar, 10 ^oC, and $[PFOS]_i = [PFOA]_i = 100$ μg L^{-1}.

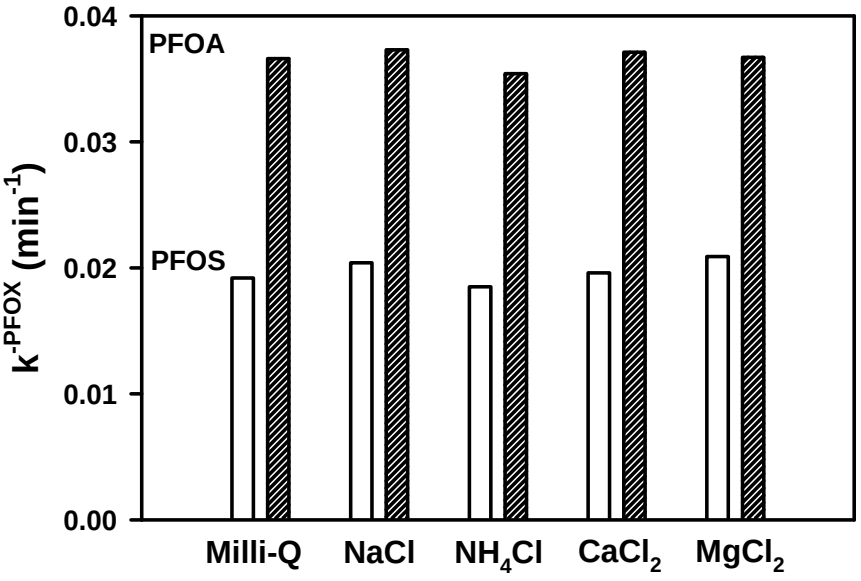

Figure 7.4. k^{-PFOX}, the pseudo-first-order rate constant for sonolysis of PFOS (○) and PFOA (▽), vs. pH of the aqueous solution. Dashed lines represent values of plus and minus one standard deviation from the mean rate constant obtained under pH 7, $k^{-PFOS} = 0.0192 \pm 0.0016$ min^{-1}, and $k^{-PFOA} = 0.0366 \pm 0.0003$ min^{-1}.

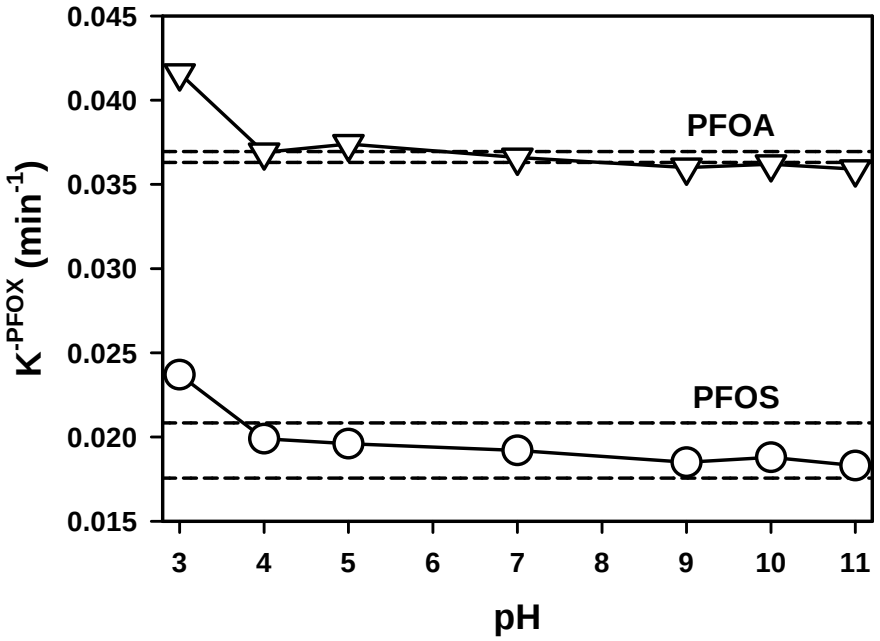

Figure 7.5. (a) $\ln([PFOS]_t / [PFOS]_i)$ and $\ln([PFOA]_t / [PFOA]_i)$ (b) vs. time in minutes during the sonolysis of PFOS and PFOA in groundwater under its original pH 8.0 (○) , pH 11.0 (□), and pH 3.9 (▽). Other reaction parameters are: 612 kHz, 250 W L^{-1}, Ar, 10 ^{o}C, and $[PFOS]_i = [PFOA]_i = 100$ μg L^{-1}.

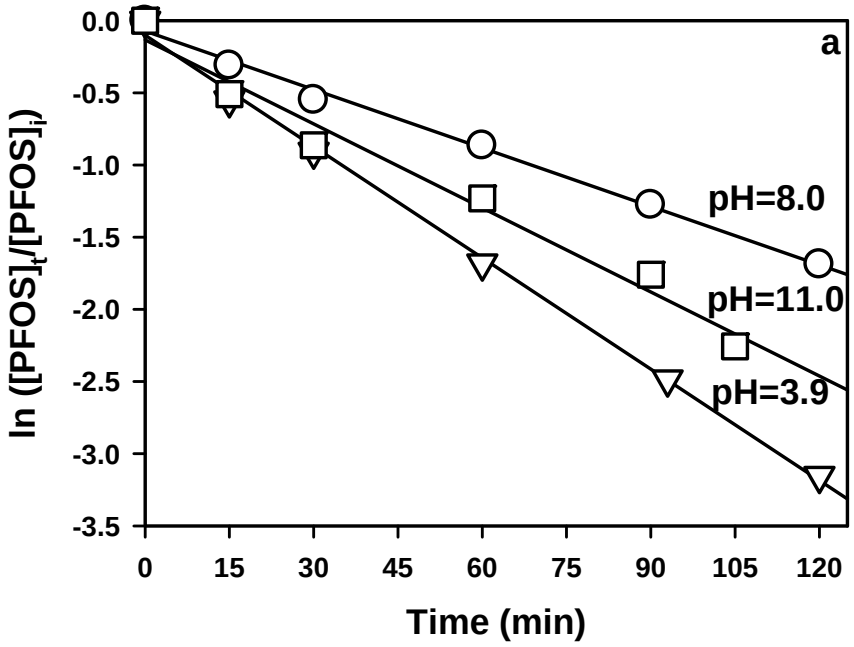

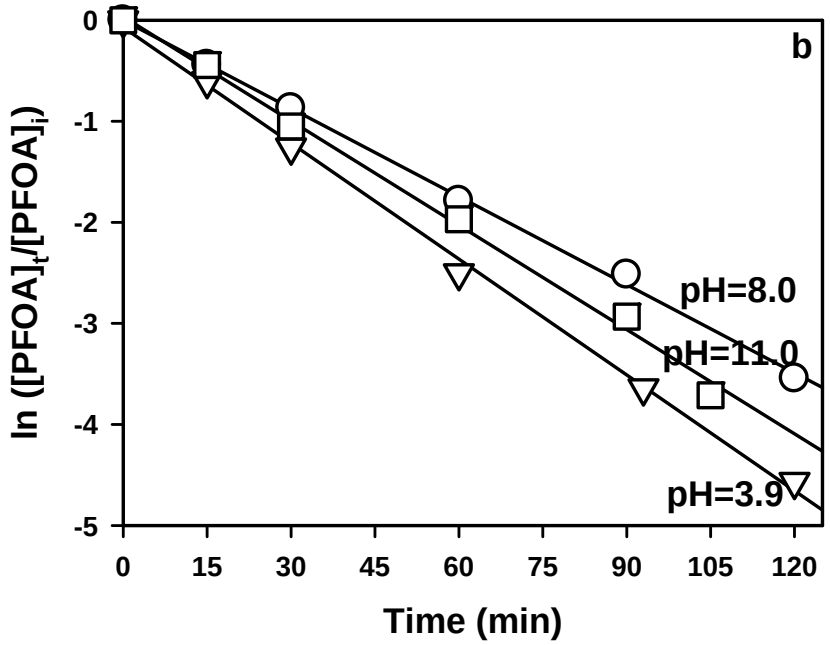

Figure 7.6. $\ln([PFOS]_t / [PFOS]_i)$ (a) and $\ln([PFOA]_t / [PFOA]_i)$ (b) vs. time in minutes during sonochemical degradation in Milli-Q water (○) and groundwater (□) under 354 kHz, 250 W L^{-1}, Ar, 10 °C for $[PFOS]_i = [PFOA]_i = 100$ μg L^{-1}. Each error bar represents one standard deviation from the mean of at least three experiments. $k_{MQ}^{-PFOS} = 0.0239$ min^{-1}, $k_{GW}^{-PFOS} = 0.0170$ min^{-1}, $k_{MQ}^{-PFOA} = 0.0469$ min^{-1}, and $k_{GW}^{-PFOA} = 0.0356$ min^{-1}.

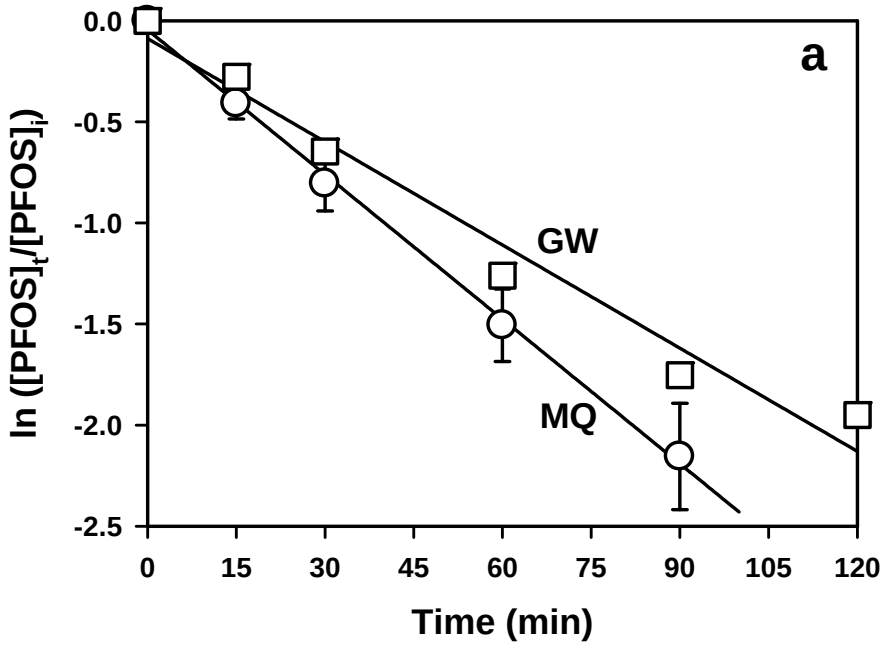

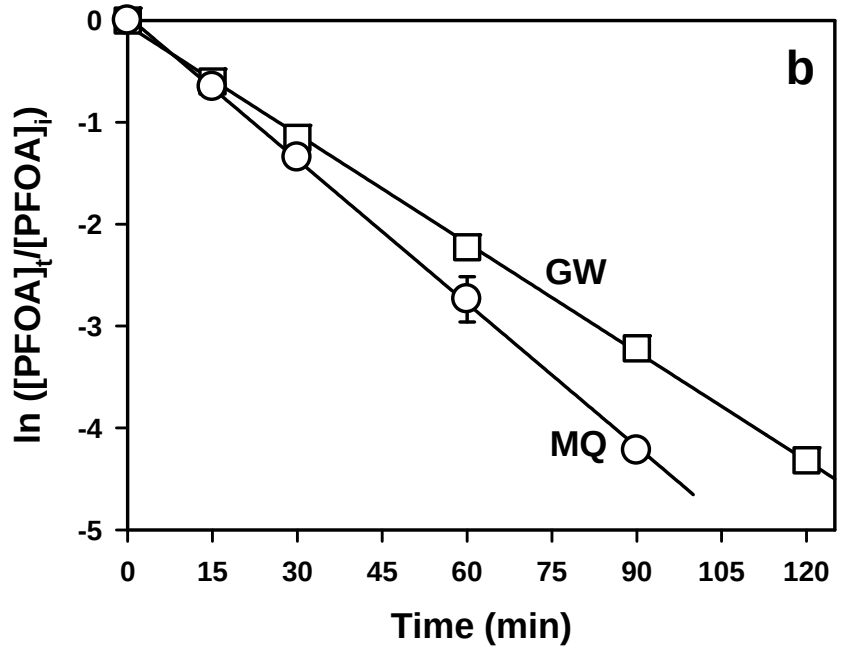

Figure 7.7. The titration curve of the groundwater sample: pH of the groundwater sample vs. the concentration of HCl added in mM.